Laser and Particle Beams (2004), *22*, 89–94. Printed in the USA.

DOI: 10.1017/S0263034604221176

Parametric up-conversion of a trivelpiece–gould mode in a beam–plasma system

D.N. GUPTA[1] AND A.K. SHARMA[2]

[1]Department of Physics, University of Rajasthan, Jaipur, India
[2]Center for Energy Studies, Indian Institute of Technology, New Delhi, India

(RECEIVED 25 July 2003; ACCEPTED 24 November 2003)

Abstract

A large amplitude Trivelpiece–Gould (TG) mode, in a strongly magnetized beam–plasma system, parametrically couples to a beam space charge mode and a TG mode sideband. The density perturbation associated with the beam mode couples with the electron oscillatory velocity, due to the pump wave, to produce a nonlinear current, driving the sideband. The pump and the sideband waves exert a ponderomotive force on the electrons with a component parallel to the ambient magnetic field, driving the beam mode. For a pump wave having $\mathbf{k}_0 \cdot \mathbf{v}_{0b}^0/\omega_0 < 0$, where ω_0, $\mathbf{k}_0$ are the frequency and the wave number of the pump, and $\mathbf{v}_{0b}^0$ is the beam velocity, the sideband is frequency upshifted. At low beam density (Compton regime) the growth rate of the parametric instability scales as two-thirds power of the pump amplitude, and one-third power of beam density. In the Raman regime, the growth rate scales as half power of beam density and linearly with pump amplitude. The background plasma has a destabilizing role on the instability.

Keywords: Beam–plasma system; Parametric up-conversion; TG mode

1. INTRODUCTION

A magnetized beam–plasma system supports a variety of electrostatic and electromagnetic modes. These modes can either be launched externally or excited in situ via linear and nonlinear mechanisms. At higher amplitudes they are coupled and can exchange energy and momentum with each other. Such nonlinear interactions are important in many laboratory experiments and space plasmas. The parametric instability in magnetized plasma is a particular type of nonlinear coherent wave phenomena (Chang *et al*., 1971).

Large amplitude Trivelpiece–Gould (TG) modes or lower hybrid waves have been observed in several experiments by using axial and spiraling electron and ion beams (Sharma *et al*., 1998; Krafft & Volokitin, 2000; Maslennikov & Stepanov, 2000; Volokitin & Krafft, 2001). Prabhuram and Sharma (1992) have observed the excitation of higher harmonics of a TG mode in a low-energy beam–plasma system. Large amplitude TG modes, also known as lower hybrid waves, have been employed for heating and for current drive in tokamak (Taylor *et al*., 1989) and suppression of microinstabilities in Q-machine (Berger *et al*., 1976; Amatucci *et al*., 1996; Koepkr, 2002, and reference therein). These waves have also been observed as a dominant instability in magnetized beam–plasma systems where they are called the TG mode (Sakawa *et al*., 1993). They give rise to a variety of nonlinear phenomena, for example, harmonic generation, modulational instability, and parametric instabilities. Liu and Tripathi (1984) and Porkolab (1974) have given a detailed survey of parametric instabilities of lower hybrid waves in tokamaks. Seiler *et al*. (1976) have reported experimental results on the excitation of a lower hybrid instability by a spiraling ion beam in the linear Princeton Q-1 device.

Plasma heating by high-energy particle-beam injection is considered to be one of the most promising methods of obtaining the ion temperatures necessary for a thermonuclear plasma. The mechanism by which the beam transfers its energy to the target plasma has been a subject of intense research (Yatsui & Imai, 1975; Porkolab *et al*., 1976). An electron beam injected parallel to the confining magnetic field of a low-β, isothermal ($T_e \approx T_i$) plasma is density modulated at or above the lower hybrid frequency (ω_{LH}) of the target plasma. Allen *et al*. (1978) have observed that such a modulation can parametrically excite a lower hybrid wave and either an ion quasimode or an ion-cyclotron mode.

Address correspondence and reprint requests to: D.N. Gupta, Department of Physics, University of Rajasthan, Jaipur, India. E-mail: dngupta2001@hotmail.com.

In this article, we study the nonlinear coupling of a large amplitude TG mode with the beam mode in a magnetized beam–plasma system. The TG mode (ω_0, $\mathbf{k}_0$), imparts oscillatory velocity to electrons that couples with the density perturbation associated with the beam mode ($\omega \approx k_z v_{0b}^0, \mathbf{b}$) to produce a nonlinear current, deriving a TG mode sideband ($\omega_1 = \omega_0 + \omega$, $\mathbf{k}_1 = \mathbf{k}_0 + \mathbf{k}$). The sideband beats with the pump to exert a parallel ponderomotive force on electrons, driving the beam mode.

In Section 2 we carry out the instability analysis following the fluid approach and obtain an expression for the growth rate of the parametric instability under beam-dominated decay (Wang *et al.*, 1996) in Compton and Raman regimes. A brief discussion of results is presented in Section 3.

2. INSTABILITY ANALYSIS

Consider a magnetized beam–plasma system with electron density n_0^0 and static magnetic field $B_s\hat{z}$. An electron beam of density n_{0b}^0 propagates through it with velocity $v_{0b}^0\hat{z}$. A large amplitude TG mode exists in the plasma. If we ignore finite boundary effects, the potential of the TG mode can be written as

$$\phi_0 = \phi_0 \exp[-i(\omega_0 t - \mathbf{k}_0\cdot\mathbf{x})], \tag{1}$$

where $\omega_0 = \omega_{1h}[1 + k_{0z}^2/k_0^2(m_i/m)]^{1/2}$, $\omega_{1h} = \omega_{pi}/(1 + \omega_p^2/\omega_c^2)^{1/2}$, $\mathbf{k}_0 = k_{0x}\hat{x} + k_{0z}\hat{z}$, ω_p and ω_c are the electron plasma and cyclotron frequencies, ω_{pi} is the ion plasma frequency, and m_i and m are the ion and electron masses, respectively.

The TG mode imparts oscillatory velocity to plasma and beam electrons. Solving the equations of motion and continuity, the velocity and density perturbations of the beam electrons can be written as

$$\mathbf{v}_{0b\perp} = -\frac{ie\phi_0}{m\omega_c^2}[(\mathbf{k}_0 \times \boldsymbol{\omega}_c) + i(\omega_0 - k_z v_{0b}^0)\mathbf{k}_{0\perp}], \tag{2}$$

$$v_{0b\parallel} = -\frac{ek_{0\parallel}\phi_0}{m(\omega_0 - k_z v_{0b}^0)}, \tag{3}$$

$$n_{0b} = -n_{0b}^0\frac{e\phi_0}{m}\left[\frac{k_{0\parallel}^2}{(\omega_0 - k_z v_{0b}^0)^2} - \frac{k_{0\perp}^2}{\omega_c^2}\right], \tag{4}$$

where subscripts $\perp$ and $\parallel$ refer to the perpendicular and parallel components with respect to magnetic field $\mathbf{B}_s$. Corresponding quantities for plasma electrons, $\mathbf{v}_0$ and n_0, can be deduced from Eqs. (2)–(4) by dropping the subscript b and taking $v_{0b}^0 = 0$. Eqs. (2) and (4) are valid for $\omega_0 \ll \omega_c$.

The pump wave decays into a low frequency electrostatic wave (beam mode) with potential $\phi(\omega, \mathbf{k})$ and a TG mode sideband wave of potential $\phi_1(\omega_1, \mathbf{k}_1)$, where $\omega_1 \equiv \omega_0 + \omega$, $\mathbf{k}_1 \equiv \mathbf{k}_0 + \mathbf{k}$. The linear response at $(\omega_1, \mathbf{k}_1)$ is the same as given by Eqs. (2)–(4), with ω_0, $\mathbf{k}_0$ replaced by ω_1, $\mathbf{k}_1$. The sideband of potential $\phi_1(\omega_1, \mathbf{k}_1)$ couples with the pump to produce a low-frequency ponderomotive force $\mathbf{F}_p = m\mathbf{v}\cdot\nabla\mathbf{v}$ on the electrons. $\mathbf{F}_p$ has two components, one perpendicular to the static magnetic field $\mathbf{B}_s$ and the other parallel to it. The response of electrons to $\mathbf{F}_{p\perp}$ is strongly suppressed by the magnetic field and is usually weak (for $\omega_p \ll \omega_c$). In the parallel direction, the electrons can effectively respond to $\mathbf{F}_{p\parallel}$; hence, the low-frequency nonlinearity arises mainly through $\mathbf{F}_{p\parallel} = -m\mathbf{v}\cdot\nabla v_\parallel$. For $\omega < k_\parallel v_{th}$ (v_{th} being the electron thermal speed), the electron can spontaneously follow the ponderomotive force and the nonlinearity is strong. At longer wavelengths $\omega > k_\parallel v_{th}$, the electrons' response in the parallel direction is slow and the nonlinearity is weak. The parallel ponderomotive force on the beam electrons can be explicitly written as

$$\mathbf{F}_{pb\parallel} = -(m/2)[\mathbf{v}_{0b\perp}^*\cdot\nabla_\perp v_{1b\parallel} + \mathbf{v}_{1b\perp}\cdot\nabla_\perp v_{0b\parallel}^*], \tag{5}$$

where we have dropped the $v_{0\parallel}\nabla_\parallel$ and $v_{1\parallel}\nabla_\parallel$ terms as these are $k_z k_{0z}\omega_0/kk_0\omega_c = (m/m_i)^{1/2}$ times the terms retained. Substituting for $v_{0b\perp}^*$ and $v_{1b\perp}^*$, and considering only dominant $\mathbf{E}\times\mathbf{B}_s$ terms, one may simplify Eq. (5) to write $\mathbf{F}_{pb\parallel} = eik_z\phi_{pb}$, where

$$\phi_{pb} = \frac{e\phi_0^*\phi_1}{2m\omega_c^2}\frac{\mathbf{k}_{1\perp}\cdot\mathbf{k}_{0\perp}\times\boldsymbol{\omega}_c}{ik_z\omega_1(\omega_0 - k_{0z}v_{0b}^0)} \times[k_z(\omega_0 - k_{0z}v_{0b}^0) - k_{0z}(\omega - k_z v_{0b}^0)]. \tag{6}$$

The ponderomotive potential ϕ_p for plasma electrons can be deduced from Eq. (6) taking $v_{0b}^0 = 0$. ϕ_{pb} and ϕ_p at $(\omega, \mathbf{k})$ produce a low-frequency beam electron density perturbation

$$n_b = \frac{k^2}{4\pi e}\chi_b(\phi + \phi_{pb}), \tag{7}$$

where $\chi_b = -\omega_{pb}^2(k_z^2/k^2)/(\omega - k_z v_{0b}^0)^2$. We neglected the role of $\mathbf{E}_\perp$ on beam electrons assuming $(\omega - k_z v_{0b}^0)^2 \ll \omega_c^2 k_z^2/k_\perp^2$.

The low-frequency plasma electron density perturbation is

$$n = \frac{k^2}{4\pi e}\chi_e(\phi + \phi_p), \tag{8}$$

where $\chi_e = -\omega_p^2(k_z^2/k^2)/\omega^2 - \omega_p^2(k_\perp^2/k^2)/\omega_c^2$ for $\omega_c \gg \omega$. Using the density perturbations in Poisson's equation, we obtain

$$\epsilon\phi = -\chi_b\phi_{pb} - \chi_e\phi_p, \tag{9}$$

where $\epsilon = 1 + \chi_e + \chi_b$. The nonlinear density perturbations n_{1b}^{NL} and n_1^{NL} at $(\omega, \mathbf{k})$ can be obtained from equation of continuity

https://doi.org/10.1017/S0263034604221176 Published online by Cambridge University Press

$$n_{1b}^{NL} = \frac{\mathbf{k}_1 \cdot \mathbf{v}_{0b}}{2\omega_1} n_b, \tag{10}$$

$$n_1^{NL} = \frac{\mathbf{k}_1 \cdot \mathbf{v}_0}{2\omega_1} n. \tag{11}$$

Using Eqs. (10) and (11) in the Poisson's equation for the sideband wave, we obtain

$$\epsilon_1 \phi_1 = -\frac{4\pi e}{k_1^2} (n_{1b}^{NL} + n_1^{NL}), \tag{12}$$

where $\epsilon_1 = 1 + \omega_p^2(k_{1\perp}^2/k_1^2)/\omega_c^2 - \omega_p^2(k_{1z}^2/k_1^2)/\omega_1^2$.

Eqs. (9) and (12) are the nonlinear-coupled equations for ϕ and ϕ_1 from which the nonlinear dispersion relation can be obtained:

$$\epsilon\epsilon_1 = \mu = \frac{k^2 c_s^2}{4\omega_1^2}\left(\frac{u^2}{c_s^2}\right)(\chi_e + \chi_b)(\chi_e \Delta_1 + \chi_b \Delta_2)\sin^2\delta_1, \tag{13}$$

where $\Delta_1 = [1 - \omega(k_{0z}/k_z)/\omega_0]$, $\Delta_2 = [1 - \omega(k_{0z}/k_z)/(\omega_0 - k_z v_{0b}^0)]$, $u = ek_0|\phi_0^*|/m\omega_c$ is the magnitude of $\mathbf{E} \times \mathbf{B}_s$ electron velocity, δ_1 is the angle between $\mathbf{k}_{1\perp}$ and $\mathbf{k}_{0\perp}$, and c_s is the sound speed.

Using $\chi_e + \chi_b + 1 \approx 0$ in Eq. (13), we get

$$\epsilon\epsilon_1 = \mu = -\frac{k^2 c_s^2}{4\omega_1^2}\left(\frac{u^2}{c_s^2}\right)(\chi_e \Delta_1 + \chi_b \Delta_2)\sin^2\delta_1.$$

In the case when ω, $\mathbf{k}$ wave is the beam mode ($\omega \approx k_z v_{0b}^0$), $\chi_b \gg \chi_e$ (beam-dominated decay), μ simplifies to

$$\epsilon\epsilon_1 = \mu = -\frac{k^2 c_s^2}{4\omega_1^2}\left(\frac{u^2}{c_s^2}\right)\chi_b \Delta_2 \sin^2\delta_1,$$

or

$$\epsilon\epsilon_1 \approx \mu \approx \frac{k_z^2 c_s^2}{4\omega_1^2}\left(\frac{u^2}{c_s^2}\right)\frac{\omega_{pb}^2}{(\omega - k_z v_{0b}^0)^2}\Delta_2 \sin^2\delta_1. \tag{14}$$

We solve Eq. (14) in two distinct cases of interest.

2.1. Compton regime

In the case when beam density (or the beam current) is small, $\chi_b \ll 1$, self-consistent potential of the beam can be neglected as compared to ponderomotive potential ($\phi \ll \phi_{pb}$), and Eq. (14) can be written as

$$(\omega - k_z v_{0b}^0)^2\left(1 - \frac{\omega_p^2}{\omega_1^2}\frac{k_{1z}^2}{k_1^2} + \frac{\omega_p^2}{\omega_c^2}\frac{k_{1\perp}^2}{k_1^2}\right) = R\omega_{pb}^2\frac{k_z^2}{k^2}$$

or

$$(\omega - k_z v_{0b}^0)^2(\omega_1^2 - \omega_{1r}^2) = R\omega_1^2\omega_{pb}^2\frac{k_z^2}{k^2}, \tag{15}$$

where $R = (k_z^2 c_s^2/4\omega_1^2)(u^2/c_s^2)\Delta_2 \sin^2\delta_1$, and $\omega_{1r}^2 = [\omega_p^2 k_{1z}^2/k_1^2 - \omega_p^2(k_{1\perp}^2/k_1^2)\omega_1^2/\omega_c^2]$.

The maximum growth rate of the instability occurs near the simultaneous zeroes of the left-hand side. Choosing $\omega = k_z v_{0b}^0 + \delta$, and $\omega_1 = \omega_{1r} + \delta$, where δ is the frequency mismatch, Eq. (15) gives

$$\delta = \left(\frac{R\omega_{1r}\omega_{pb}^2 k_z^2}{2k^2}\right)^{1/3} e^{i2\pi 1/3},$$

where $1 = 0, 1, 2$. The growth rate turns out to be

$$\gamma = Im(\delta) = \frac{\sqrt{3}}{2}\left(\frac{R\omega_{1r}\omega_{pb}^2 k_z^2}{2k^2}\right)^{1/3}. \tag{16}$$

Because $\mathbf{k}_1 = \mathbf{k}_0 + \mathbf{k}$ and $\omega_1 = \omega_0 + \omega$, we get

$$k^2 = k_{0z}^2\frac{\omega_0^2}{\omega_p^2} + (k_{0z} + k_z)^2\frac{(\omega_0 + k_z v_{0b}^0)^2}{\omega_p^2} + k_z^2. \tag{17}$$

The growth rate of the parametric instability scales as two-thirds power of the pump amplitude and one-third power of beam density. This treatment, however, is valid when $\gamma^2 > \omega_{pb}^2$ (weak beam limit).

To calculate the normalized growth rate γ/ω_{pb} in a Compton regime, we estimate k/k_{0z} for different values of $k_z/k_{0z} = 0$, 0.2, 0.4, 0.6, 0.8, 1.0 from Eq. (17) first. Using $\omega_1 = \omega_p k_{1z}/k_1$ (for TG mode sideband), $\omega_1 = \omega_0 - \omega$, $k_{1z} = k_{0z} - k_z$, and $\omega = k_z v_{0b}^0$ (for beam mode), we calculate the normalized growth rate from Eq. (16).

In Figure 1, we have plotted the normalized growth rate γ/ω_{pb} of the parametric instability in the Compton regime as a function of the normalized parallel wave number of the beam mode k_z/k_{0z} for upper sideband generation in a beam–plasma system. The parameters are $-v_{0b}^0/c = 0.1$, $k_{0z}c/\omega_0 = 3$, $c_s/c = 10^{-5}$, $\delta_1 = \pi/2$, $u^2/c_s^2 = 1$, $\omega_{pb}/\omega_p = 0.2$, and $\omega_0/\omega_p = 0.1$, 0.2. The normalized growth rate of the parametric instability in the Compton regime increases with the normalized wave number of the beam mode. One may also see that for a pump wave counterpropagating with the beam, the sideband is frequency upshifted, whereas, for copropagating with a beam, the sideband is frequency downshifted. Figure 1 also shows the effect of background plasma on the growth rate of instability. The rate of growth increases with background plasma density.

2.2. Raman regime

At high beam density, one may have $\epsilon \approx 0$. In this case, self-consistent potential far exceeds the ponderomotive one ($\phi \gg \phi_{pb}$). Then one looks for a solution of Eq. (14) around

https://doi.org/10.1017/S0263034604221176 Published online by Cambridge University Press

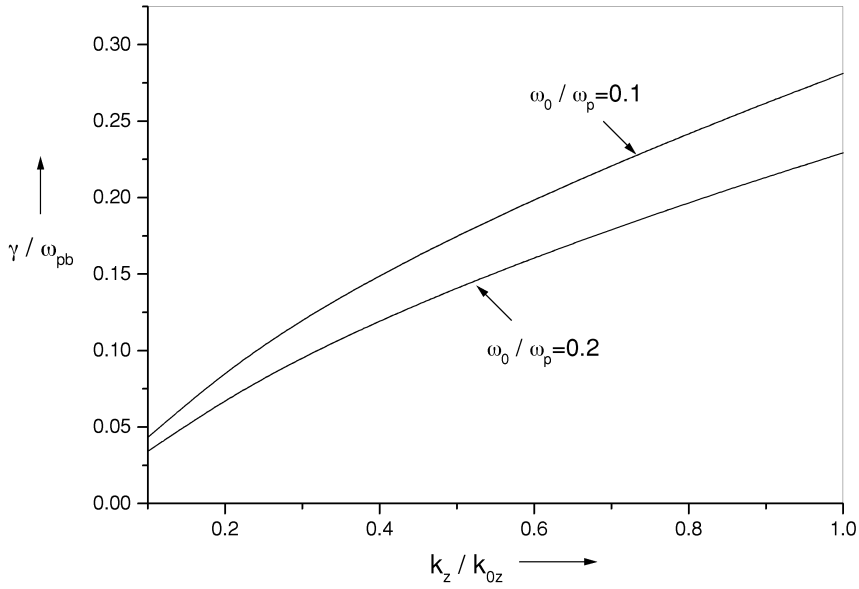

Fig. 1. Variation of the normalized growth rate of the parametric instability in the Compton regime as a function of the normalized parallel wave number of the beam mode. The parameters are $-v_{0b}^0/c = 0.1$, $k_{0z}c/\omega_0 = 3$, $c_s/c = 10^{-5}$, $\delta_1 = \pi/2$, $u^2/c_s^2 = 1$, $\omega_{pb}/\omega_p = 0.2$, and $\omega_0/\omega_p = 0.1, 0.2$.

the simultaneous zeroes of the left-hand side. Eq. (14) takes the form

$$\left[1 - \frac{\omega_{pb}^2}{(\omega - k_z v_{0b}^0)^2}\frac{k_z^2}{k^2} - \frac{\omega_p^2}{\omega^2}\frac{k_z^2}{k^2}\right] \times \left(1 - \frac{\omega_p^2}{\omega_1^2}\frac{k_{1z}^2}{k_1^2} + \frac{\omega_p^2}{\omega_c^2} + \frac{\omega_p^2}{\omega_c^2}\frac{k_{1\perp}^2}{k_1^2}\right) = R$$

or

$$(\omega^2 - \omega_r^2)(\omega_1^2 - \omega_{1r}^2) = R\,\frac{\omega_1^2(\omega - k_z v_{0b}^0)^2}{(1 - \omega_p^2 k_z^2/\omega^2 k^2)}, \tag{18}$$

where

$$\omega_r = k_z v_{0b}^0 - \frac{\omega_{pb} k_z/k}{(1 - \omega_p^2 k_z^2/\omega^2 k^2)^{1/2}}.$$

We choose $\omega = \omega_r + \delta$ and $\omega_1 = \omega_{1r} + \delta$ for maximum growth and solve Eq. (18) for δ. The growth rate turns out to be

$$\gamma = Im(\delta) = \frac{1}{4}\,\frac{\omega_{pb} k_z/k}{(1 - \omega_p^2 k_z^2/\omega^2 k^2)}\left(\frac{R\omega_{1r}}{\omega_r}\right)^{1/2}, \tag{19}$$

where

$$k^2 = k_{0z}^2\frac{\omega_0^2}{\omega_p^2} + (k_{0z} + k_z)^2 \times \left[\frac{k_z v_{0b}^0}{\omega_p} - \frac{\omega_{pb} k_z/\omega_p k}{(1 - \omega_p^2 k_z^2/\omega^2 k^2)^{1/2}}\right]^{1/2} + k_z^2, \tag{20}$$

from phase matching conditions.

The growth rate of the parametric instability scales as half power of beam density and linearly with pump amplitude. This theory is also applicable for lower sideband generation when the beam travels along the direction of the pump wave.

We calculate the normalized growth rate γ/ω_{pb} in the Raman regime from Eqs. (19) and (20) by using the mathematical method used in the Compton regime.

In Figure 2 we have plotted the growth rate in the Raman regime as a function of k_z/k_{0z} for the corresponding value of $\omega_{pb}/\omega_p = 0.5$. The normalized growth rate increases with the normalized parallel wave number of the beam mode k_z/k_{0z}. The background plasma plays a significant role and enhances the growth rate of the instability.

3. DISCUSSION

A nonlinear dispersion relation describing three-wave interaction and instability growth rates are found. The theoretical results obtained above are applicable to the explanation of phenomena observed in laboratory plasmas as well as in space plasmas. We present the theory on parametric instabilities in space-charge-dominated beams, which are important to the design and development of induction accelerators as heavy ion fusion drivers (Wang *et al.*, 1996).

A large amplitude TG mode propagating through a magnetized plasma, in the presence of an electron beam, undergoes parametric coupling with a negative energy beam space charge mode and a TG mode sideband. For $\omega \approx k_z v_{0b}^0$, the coupling is caused by a ponderomotive-force-driven beam mode and one obtains upper sideband generation. However, in the Raman regime, one obtains an upper sideband for $\omega < k_z v_{0b}^0$. The sideband frequency is upshifted for the

https://doi.org/10.1017/S0263034604221176 Published online by Cambridge University Press

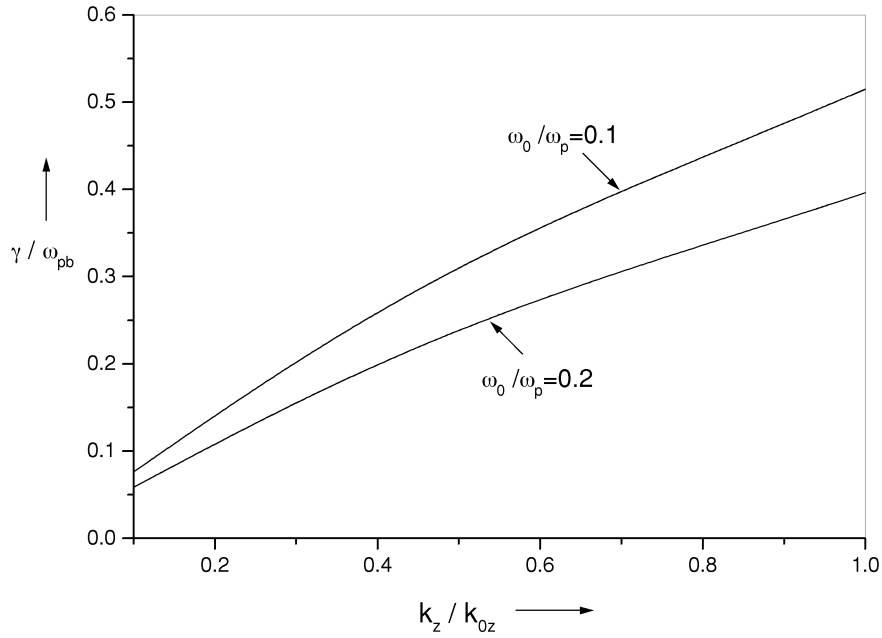

Fig. 2. Variation of the normalized growth rate of the parametric instability in the Raman regime as a function of the normalized parallel wave number of the beam mode for the same parameters as those in Figure 1 and $\omega_{pb}/\omega_p = 0.5$.

negative energy beam space charge mode. The presence of plasma enhances the growth rate of the up-conversion process.

For a low-density beam the growth rate of the parametric instability scales as two-thirds power of the pump amplitude and one-third power of the beam density, whereas, in the case of a high-density beam the rate of growth of the parametric instability scales as half power of beam density and linearly with pump amplitude. Hence, the beam density enhances the rate of growth of the parametric instability in a beam–plasma system.

The two-stream instability competes with this instability. The former has a growth rate $\gamma_T \approx \sqrt{3}/2(\omega_{pb}^2\omega_p/2)^{1/3}$ that may be higher than the growth rate of the parametric instability. The parametric instability would then arise after the two-stream instability has been saturated. However, the beam would acquire a finite velocity spread due to the two-stream instability, and one must employ a kinetic theory for the parametric coupling. Stimulated Compton scattering may be suppressed totally by kinetic effects but the stimulated Raman scattering would exist with roughly the same growth rate as above. Obiki *et al*. (1967) have reported an experimental study of suppression of a two-stream instability in a beam–plasma system by external ac electric fields. Davydova *et al*. (1986) have shown theoretically that a nonuniform external rf field can suppress a resonant instability of TG waves excited by a monoenergetic electron beam. In these situations, the parametric instability discussed above could be prominent.

ACKNOWLEDGMENT

D.N. Gupta is grateful to Professor V.K. Tripathi for stimulating and valuable discussion.

REFERENCES

Allen, G.R., Owens, D.K., Seiler, S.W., Yamada, M., Ikezi, H. & Porkolab, M. (1978). Parametric lower-hybrid instability driven by modulated electron-beam injection. *Phys. Rev. Lett.* **41**, 1045–1048.

Amatucci, W.E., Walker, D.N., Ganguli, G., Antoniades, J.A., Duncan, D., Bowles, J.H., Gavrishchaka, V. & Koepke, M.E. (1996). Plasma response to strongly sheared flow. *Phys. Rev. Lett.* **77**, 1978–1981.

Berger, R.L., Chen, L., Kaw, P.K. & Perkins, F.W. (1976). Lower hybrid parametric instabilities-nonuniform pump waves and tokamak applications. *Phys, Fluids* **20**, 1864–1875.

Chang, J., Raether, M. & Tanaka, S. (1971). Experimental observation of wave-wave coupling in a beam-plasma system. *Phys. Rev. Lett.* **27**, 1263–1266.

Davydova, T.A., Lashkin, V.M, Shamrai, K.P. (1986). Effect of external rf field on instability of Trivelpiece-Gould waves in a plasma with an electron beam. *Sov. J. Plasma Phys* **12**, 235–237.

Koepkr, M.E. (2002). Contributions of Q-machine experiments to understanding auroral particle acceleration processes. *Phys. Plasmas* **9**, 2420–2427, and reference therein.

Krafft, C., Volokitin, A.S. & Fle, M. (2000). Nonlinear electron beam interaction with a whistler wave packet. *Phys. Plasmas* **7**, 4423–4432.

https://doi.org/10.1017/S0263034604221176 Published online by Cambridge University Press

Liu, C.S., Tripathi, V.K., Chan, V.S. & Stefan, V. (1984). Density threshold for parametric instability of lower-hybrid waves in tokamaks. *Phys. Fluids* **27**, 1709–1717.

Maslennikov, D.I., Mikhailenko, V.S. & Stepanov, K.N. (2000). Decay instability of a lower hybrid wave. *Plasma Physics Report* **26**, 139–146.

Obiki. T., Itatani, R. & Otani, Y. (1968). Suppression of a two-stream interaction in a beam-plasma system by external ac electric fields. *Phys. Rev. Lett.* **20**, 184–187.

Porkolab, M. (1974). Theory of parametric instability near the lower-hybrid frequency. *Phys. Fluids* **17**, 1432–1442.

Porkolab, M., Bernabei, S., Hooke, W.M., Motley, R.W. & Nagashima, T. (1977). Observation of parametric instabilities in lower-hybrid radio frequency heating of tokamaks. *Phys. Rev. Lett.* **38**, 230–233.

Prabhuram, G. & Sharma, A.K. (1992). Second harmonic excitation of TG mode in a beam plasma system. *J. Plasma Phys.* **48**, 3–12.

Sakawa, Y., Joshi, C., Kaw, P.K., Chen, F.F., Jain, V.K. (1993). Excitation of the modified Simon–Hoh instability in an electron beam produced plasma. *Phys. Fluids* **B5 (6)**, 1681–1694.

Seiler, S., Yamada, M. & Ikezi, H. (1976). Lower hybrid instability driven by a spiraling ion beam. *Phys. Rev. Lett.* **37**, 700–703.

Sharma, S.C., Srivastava, M.P., Sugawa, M. & Tripathi, V.K. (1998). Excitation of lower hybrid waves by a density-modulated electron beam in a plasma cylinder. *Phys. Plasmas* **5**, 3161–3164.

Taylor, R.J., Brown, M.L., Fried, B.D., Grote, H., Liberati, J.R., Morales, G.J., Pribyl, P., Darrow, D. & Ono, M. (1989). *H*-mode behavior induced by cross-field currents in a tokamak. *Phys. Rev. Lett.* **63**, 2365–2368.

Volokitin, A.S. & Krafft, C. (2001). Electron beam interaction with lower hybrid waves at Cherenkov and cyclotron resonances. *Phys. Plasmas* **8**, 3748–3758.

Wang, J.G., Suk, H. & Reiser, M. (1996). Experimental studies of space-charge waves and resistive-wall instability in space-charge-dominated electron beams. *Fusion Engineering and Design* **32–33**, 141–148.

Yatsui, K. & Imai, T. (1975). Plasma heating by lower-hybrid parametric instability pumped by an electron beam. *Phys. Rev. Lett.* **35**, 1279–1282.